ORIGINAL ARTICLE

Lung structure and function on MRI in preterm born school children with and without BPD: A feasibility study

Bernadette B. L. J. Elders[1,2] | Harm A. W. M. Tiddens[1,2] |
Mariëlle W. H. Pijnenburg[1] | Irwin K. M. Reiss[3] | Piotr A. Wielopolski[2] |
Pierluigi Ciet[1,2]

[1]Department of Paediatric Pulmonology and Allergology, Erasmus MC—Sophia Children's Hospital, University Medical Centre Rotterdam, Rotterdam, The Netherlands

[2]Department of Radiology and Nuclear Medicine, Erasmus MC—Sophia Children's Hospital, University Medical Centre Rotterdam, Rotterdam, The Netherlands

[3]Department of Neonatology, Erasmus MC—Sophia Children's Hospital, University Medical Centre Rotterdam, Rotterdam, The Netherlands

Correspondence
Pierluigi Ciet, Department of Radiology and Nuclear Medicine, Erasmus MC—Sophia Children's Hospital, University Medical Centre Rotterdam, Wytemaweg 80, Rotterdam 3015CN, The Netherlands.
Email: p.ciet@erasmusmc.nl

Abstract

Background and Objective: The most common respiratory complication of prematurity is bronchopulmonary dysplasia (BPD), leading to structural lung changes and impaired respiratory outcomes. However, also preterm children without BPD may show similar adverse respiratory outcomes. There is a need for a safe imaging modality for preterm children with and without BPD for disease severity assessment and risk stratification. Our objective was to develop a magnetic resonance imaging (MRI) protocol in preterm children with and without BPD at school age.

Methods: Nine healthy volunteers (median age 11.6 [range: 8.8–12.8] years), 11 preterm children with BPD (11.0 [7.2–15.6] years), and 9 without BPD (11.1 [10.7–12.6] years) underwent MRI. Images were scored on hypo- and hyperintense abnormalities, bronchopathy, and architectural distortion. MRI data were correlated to spirometry. Ventilation and perfusion defects were analyzed using Fourier Decomposition (FD) MRI.

Results: On MRI, children with BPD had higher %diseased lung (9.1 (interquartile range [IQR] 5.9–11.6)%) compared to preterm children without BPD (3.4 (IQR 2.5–5.4)%, $p < 0.001$) and healthy volunteers (0.4 (IQR 0.1–0.8)%, $p < 0.001$). % Diseased lung correlated negatively with %predicted FEV_1 ($r = -0.40$, $p = 0.04$), FEV_1/FVC ($r = -0.49$, $p = 0.009$) and FEF_{75} ($r = -0.63$, $p < 0.001$). Ventilation and perfusion defects on FD sequence corresponded to hypointense regions on expiratory MRI.

Conclusion: Chest MRI can identify structural and functional lung damage at school age in preterm children with and without BPD, showing a good correlation with spirometry. We propose MRI as a sensitive and safe imaging method (without ionizing radiation, contrast agents, or the use of anesthesia) for the long-term follow-up of preterm children.

KEYWORDS
bronchopulmonary dysplasia, imaging, MRI, paediatric, spirometry

1 | INTRODUCTION

Respiratory problems related to premature birth can lead to life-long morbidity.[1–3] The most common respiratory complication of extreme prematurity is bronchopulmonary dysplasia (BPD), leading to structural lung changes and impaired respiratory outcomes. However, also patients born extremely preterm without BPD may show similar adverse respiratory outcomes, leading to life-long morbidity.[2–5] To date, little is known about the long-term follow-up of prematurity-related lung disease and the role imaging could play in monitoring children with BPD. Computed tomography (CT) is the current gold standard to assess structural lung changes seen in children with BPD.[6] Studies have shown that structural lung abnormalities on CT have a high predictive value of short and long-term adverse respiratory outcomes in preterm patients.[7–9] However, the use of CT remains limited for radiation safety reasons, but also because CT imaging does not necessarily change the management of BPD. For these reasons, the European Respiratory Society (ERS) Task Force on long-term management of BPD has recently suggested the use of lung imaging only in subgroups of children with clinically severe BPD.[10]

Magnetic resonance imaging (MRI) can overcome the limitation related to radiation exposure and has the additional benefit of assessing both lung structure and function in a single examination, as shown for several other pediatric lung diseases.[11,12] The development of MRI as a safe and feasible imaging method for preterm-born children has great potential to identify those patients at risk for pulmonary morbidity. However, MRI research in this population is limited. Only two studies have been done in school-age children with BPD, in which hyperpolarized ^{3}He diffusion-weighted MRI was used, showing contradictory results about alveolar enlargement.[13] A disadvantage of ^{3}He diffusion-weighted MRI is the high costs of the technique, related to the hyperpolarized gases and the need for dedicated MRI scanner hardware. In neonatal BPD, multiple studies have shown good feasibility of MRI without the use of contrast agents to visualize differences in structural lung changes between healthy volunteers, and preterm-born children with and without BPD.[14–18] However, these studies focused on the short-term outcomes and were done on a unique small-footprint MRI scanner using in-house developed sequences, thus making the MRI protocol not easily implementable at other institutions. To date, no studies have been conducted using conventional MRI sequences in older children with BPD, nor in preterm-born children without BPD.

In this study, we aimed to develop a chest MRI protocol, on a standard 1.5 Tesla MRI scanner, to assess lung structure and function in preterm-born children with and without BPD at school age and to validate MRI findings against spirometry.

2 | METHODS

All children followed at the BPD outpatient clinic with severe BPD diagnosed at 36 weeks of gestational age (GA) according to the National Health Institute (NHI) criteria,[19] with an age between 6 and 16 years were approached to participate in this study. Children with BPD were compared to preterm-born children (<28 weeks postmenstrual age) without BPD or other lung pathology, randomly selected from the general neonatal follow-up clinic, and healthy volunteers (born > 37 weeks postmenstrual age) consisting of siblings or friends of the preterm-born children within the same age range. In- and exclusion criteria are shown in Supporting Information: 1. Approval was obtained from the local medical ethics committee (MEC2018-134 and MEC2018-002) and written informed consent was obtained from parents/legal representatives of all study participants.

All study participants underwent spirometry and spirometer-controlled chest MRI using the BPD protocol, except for two healthy volunteers included from a different study using a similar MRI protocol, in whom only the structural MR imaging was performed. From all preterm-born children with and without BPD, clinical data on GA, birth weight, and respiratory support during the neonatal period were retrieved from the electronic patient dossier.

2.1 | Spirometry

Flow volume curves were obtained from all study participants according to ERS/American Thoracic Society (ATS) guidelines.[20,21] Forced vital capacity (FVC), forced expiratory volume in 1 s (FEV_1), and forced expiratory flow at 75% of VC (FEF_{75}) are presented as percentage predicted and z-scores as reported by the Global Lung function Initiative.[22]

2.1.1 | MRI

A chest MRI protocol was developed on a 1.5 T MRI (Artist, GE Healthcare) using a 32 channels torso coil. The protocol consisted of breath-hold isotropic sagittal 3D proton density (PD) weighted spoiled gradient echo sequences (SPGR) images during inspiration and expiration, a respiratory navigated axial 2D T2-weighted fat-suppressed Periodically Overlapping ParalLEL Lines with Enhanced Reconstruction (PROPELLER) and a 3D PD-weighted respiratory navigated axial zero echo time (ZTE) and/or respiratory-gated ultrashort echo time (UTE) sequence during free-breathing. In addition, a 2D SPGR multiphase free-breathing sequence covering the entire thorax with 7–10 coronal slabs according to chest size with a slice thickness of 15 mm was performed for Fourier Decomposition (FD) imaging. The total protocol duration was 20–30 min, no sedation was used. Parameters of the MRI protocol are shown in Supporting Information: 2.

2.2 | Qualitative MRI analyses

Image quality was assessed using a modified version of the scoring method from Bae et al.[23] All sequences were scored on the depiction

of fissures, intrapulmonary vessels and bronchi, presence of noise/artifacts, and overall acceptability. Artifacts were further classified into blurring, streaking, wrapping, and artifacts related to low signal-to-noise ratio (SNR). Supporting Information 3 shows the scoring method, including examples of the artifacts.

2.3 | Quantitative MRI analyses

For the quantitative analyses of the MR images, a grid-based annotation method based on the PRAGMA-BPD method was developed: the bronchopulMonary rottErdam mRi morpholoGy scorE (MERGE).[9,24] An in-house developed software was used for the analysis. In this method, a grid is placed over 20 equidistant axial (reconstructed) images. The size of the grid corresponds to the largest airway diameter. Each grid is colored for BPD-related abnormalities or normal lung tissue, in a hierarchical order of clinical relevance as described in previous CT studies.[9] We identified three categories of abnormalities: hypointensity, representing CT hypoattenuation areas of mosaic perfusion, emphysema, trapped air, bullae, and cysts; hyperintensity, representing CT hyperattenuation areas of consolidation, atelectasis, and linear/subpleural opacities and bronchopathy, consisting of bronchial wall thickening and bronchiectasis. Each category was expressed as a percentage of the total lung volume. Due to the superiority of certain sequences in the identification of specific abnormalities,[11] the sequence with the highest percentage per abnormality was chosen for analyses. Figure 1 shows an example of the annotated abnormalities on the MR images from our protocol.

MERGE scoring was done in random order on all anonymized SPGR expiratory, PROPELLER, and ZTE/UTE sequences by a trained researcher with 4 years of experience in chest MRI (B. E.). Data are presented as the highest percentage for an abnormality on any of the sequences. The same researcher repeated the MERGE score on the MRIs of seven ($n = 7$; 24% of the MRI data) study participants to assess intraobserver variation of the MRI scoring, with a 4-week interval to prevent recall bias. The researcher was trained to perform the MERGE scoring by a training and test batch of example MRIs.

In addition, the degree of anatomical architecture distortion (AAD), defined as abnormal displacement of bronchi, vessels, fissures, and/or septa, was scored by counting the number of lung segments showing signs of AAD. Considering 10 segments for the right lung and 9 for the left lung.[24,25] AAD was scored as mild, moderate, and severe, when presenting in less than 7, between 7 and 13, and more than 13 lung segments, respectively.

2.4 | Ventilation and perfusion

An in-house developed algorithm based on the work of Voskrebenzev and colleagues[26-28] was used to analyze the FD images. The algorithm first corrects for intensity and registers all the images, after which a spectral decomposition of the signal is applied, separating the components of the signal related to ventilation and perfusion. Then algebraic operations allow to reconstruct ventilation and perfusion maps. This method relays on the periodic variation in signal intensity related to ventilation and perfusion, by detecting the frequency of this variation, the two components can be separated. As exploratory analyses, a visual comparison was made between the
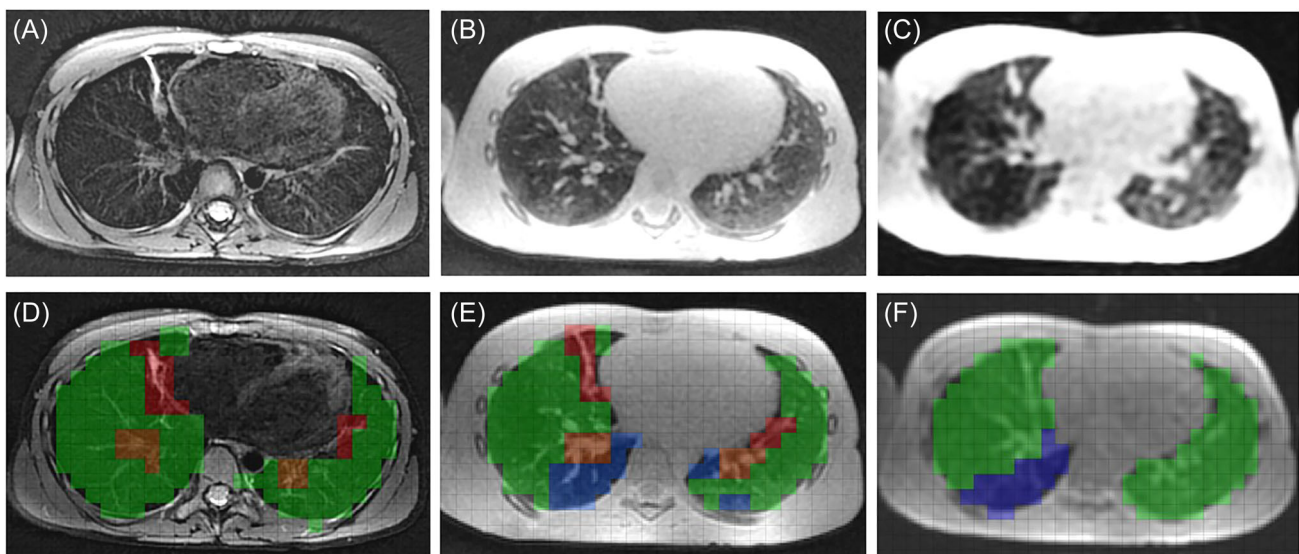
FIGURE 1 Example of the MERGE score on the MRI of an 8-year-old girl with severe BPD. (A) The axial PROPELLER, (B) ZTE, and (C) Expiratory SPGR images and corresponding MERGE scoring; (D)–(F) showing normal lung tissue (green), hyperintensity (red), hypointensity (blue), and bronchopathy (orange). BPD, bronchopulmonary dysplasia; MRI, magnetic resonance imaging; PROPELLER, periodically rotated overlapping parallel lines with enhanced reconstruction; SPGR, spoiled gradient echo; ZTE, zero echo time. [Color figure can be viewed at wileyonlinelibrary.com]

coronal reformatted SPGR expiration sequence and the ventilation and perfusion maps to classify hypo- and hyperintense regions as ventilation or perfusion defects.

2.5 | Statistics

Data analysis was done using SPSS Statistics (version 25, IBM SPSS). Parametric data are presented as mean ± standard deviation and nonparametric data are presented as median (range or interquartile range). Data were compared using the parametric t-test for normally distributed data and the Mann–Whitney U-test for not normally distributed data. Similarly, Pearson's and Spearman's ρ correlations were calculated for normally and not normally distributed data, respectively. A 5% significance level was assumed. Intraobserver agreement was calculated with the intraclass correlation coefficient and interpreted as poor (<0.50), moderate (0.50–0.75), good (0.75–0.90), or excellent (>0.90).

3 | RESULTS

Characteristics of study participants, data on respiratory support during the neonatal period, and spirometry outcomes are shown in Table 1. In total, 11 children with severe BPD, 9 preterm-born children without BPD, and 9 healthy volunteers were included with a median age of 11.0 (range: 7.2–15.6), 11.1 (range: 10.7–12.6), and 11.6 (range: 8.8–12.8) years, respectively. Children with BPD were born after a mean GA of 27.3 ± 2.4 weeks, and preterm-born children after a GA of 28.1 ± 1.4 weeks, which did not differ significantly ($p = 0.23$). In none of the electronic patient files the exact duration of respiratory support was documented, except for the type and amount of respiratory support at the time of BPD diagnosis.

3.1 | Spirometry

Children with BPD showed a significantly lower FEV_1, FEV_1/FVC, and FEF_{75} compared to preterm-born children and healthy volunteers (all $p < 0.01$) (Table 1). No significant difference in spirometry outcomes between preterm-born children and healthy volunteers was found.

3.2 | Qualitative MRI analyses

MRI was successfully performed in 28 out of 29 study subjects (97%). One subject at age of 7 years was not able to execute the full MRI protocol due to claustrophobia. Qualitative scoring results of the MR scans are shown in Table 2. The best overall image quality was achieved for the UTE, T2 weighted PROPELLER, and ZTE sequences, with an "above average" score for all. Visibility of BPD-related lung abnormalities, expressed as the disease percentage of total lung volume scored per sequence, was highest on ZTE/UTE for

hypointensity and bronchopathy, and on PROPELLER for hyperintensity (Supporting Information: 4).

The most common image artifacts were blurring for the SPGR inspiration (27.5%) and expiration (37.9%) sequences, streaking for the PROPELLER (34.5%) sequences, and low SNR for the ZTE/UTE (20.7%) sequences. However, with a minimal "satisfactory" acceptability score, these artifacts did not interfere with the assessment of MR images, which were all considered of diagnostic quality.

3.3 | Quantitative MRI analyses

MERGE and AAD results are shown in Table 3. Figure 2 shows example images of a child with BPD. The most common MRI findings in children with BPD were bronchopathy (mainly bronchial wall thickening) and hyperintensity (mainly linear opacities), while bronchopathy was the most common MRI finding in preterm-born children without BPD. Children with BPD showed, compared to preterm-born children and healthy volunteers, a significantly higher percentage of hyperintensity ($p = 0.004$ and $p < 0.001$), bronchopathy ($p = 0.002$ and $p < 0.001$), and total diseased lung ($p < 0.001$ and $p < 0.001$) on the free-breathing sequences. Hypointensity on the expiratory images was significantly higher in children with BPD compared to healthy volunteers ($p = 0.03$), but not compared to preterm-born children without BPD ($p = 0.55$). On MRI, preterm children without BPD compared to healthy volunteers showed a significantly higher percentage of all abnormalities except for the percentage of hypointense regions on free-breathing sequences (p-values all between 0.01 and 0.001). In addition, the expiratory images of preterm-born children without BPD scored higher on hypointense regions than of healthy volunteers ($p = 0.01$).

Correlations between the quantitative MRI scores and spirometry outcomes are shown in Table 4 and Supporting Information: 5. A significant negative correlation was found between the percentage of the diseased lung on MRI and the percentage predicted of FEV_1 ($p = 0.04$), FEV_1/FVC ($p = 0.009$), and FEF_{75} ($p < 0.001$), as well as between a higher score of AAD and lower spirometry outcomes (all $p < 0.001$).

The intracorrelation coefficient for MERGE outcomes on the free-breathing sequences was 0.77 for hypointensity, 0.90 for hyperintensity regions, and 0.74 for bronchopathy. Scoring of the hypointense regions on the expiratory sequence resulted in an intracorrelation coefficient of 0.94.

3.4 | Ventilation and perfusion

As an exploratory analysis, a visual comparison was made between the hypointense regions on the coronal reformatted SPGR expiration sequence and the ventilation and perfusion maps from the FD analyses in the central portion of the lung for preterm-born children with and without BPD. Two children with BPD and one preterm-born child without BPD did not have FD images of sufficient quality. In our

TABLE 1 Characteristics and spirometry outcome of all study participants

	BPD (n = 11)	Preterm(n = 9)	Healthy volunteers (n = 9/7)	p Value
Age at MRI (years, range)	11.0 (7.2–15.6)	11.1 (10.7–12.6)	11.6 (8.8–12.8)	
Gender (% female)	18.2	66.7	55.6	
PMA (weeks)	27.3 ± 2.4	28.1 ± 1.4		0.23[1]
Birth weight (grams)	910 ± 347	1106 ± 295		**0.02**[1]
Antenatal corticosteroids (n/%)	Complete 5/45 Incomplete 3/27 None 2/18 Unknown 1/9	Complete 7/78 None 2/22		
Surfactant treatment (n/%)	Yes 6/55 No 3/27 Unknown 2/18	Yes 3/33 No 6/66		
Postpartum medication				
Diuretics	Yes 8/73 No 2/18 Unknown 1/9	No 9/100		
Corticosteroids	Yes 4/36 No 5/45 Unknown 2/18	No 9/100		
Oxygen at 6 months GA	Yes 2/18 No 7/64 Unknown 2/18	No 9/100		
FVC				
% predicted	100 (94–104)	99 (95–106)	102 (73–115)	0.77[1], 0.66[2], 0.87[3]
z-score	0.0 (−0.5 to −0.3)	−0.1 (−0.5–0.5)	0.2 (−2.3–1.3)	0.66[1], 0.66[2], 0.87[3]
FEV_1				
% predicted	87 (70–89)	99 (90–104)	104 (79–109)	**0.003**[1], 0.07[2], 0.52[3]
z-score	−1.1 (−2.4 to −1.0)	−0.1 (−0.9–0.4)	0.3 (−1.8–0.8)	**0.006**[1], 0.07[2], 0.60[3]
FEV_1/FVC				
% predicted	84 (69–90)	96 (90–105)	99 (89–105)	**0.01**[1], **0.006**[2], 0.92[3]
z-score	−2.2 ± 1.1	−0.3 ± 1.4	−0.2 ± 1.1	**0.005**[1], **<0.001**[2], 0.53[3]
FEF_{75}				
% predicted	52 ± 25	91 ± 21	91 ± 20	**0.002**[1], **0.001**[2], 0.60[3]
z-score	−1.7 (−2.7 to −1.2)	−0.2 (−1.0– 0.4)	0.0 (−0.3–0.3)	**0.002**[1], **0.004**[2], 0.60[3]
VCmax				
% predicted	100 (94–104)	99 (95–107)	102 (73–115)	0.71[1], 0.66[2], 0.87[3]
z-score	0.0 (−0.5–0.3)	−0.1 (−0.5–0.6)	0.2 (−2.3–1.3)	0.66[1], 0.66[2], 0.87[3]

Note: Data are presented as mean ± standard deviation or median (range or interquartile range); $p < 0.05$ is in bold, 1 = children with BPD compared to preterm-born children without BPD, 2 = children with BPD compared to healthy volunteers, 3 = preterm-born children without BPD compared to healthy volunteers.

Abbreviations: BPD, bronchopulmonary dysplasia; FEF_{75}, forced expiratory flow at 75% of expiration; FEV_1, forced expiratory volume in 1 s; FVC, forced vital capacity; GA, gestational age; MRI, magnetic resonance imaging; PMA, postmenstrual age; VCmax, maximum vital capacity.

BPD population, two children showed a ventilation defect, one child showed a combined ventilation and perfusion defect, and one child showed two defects, one ventilation and one perfusion defect. In our preterm population without BPD, two children showed a ventilation defect. Five children with BPD and six preterm-born children without BPD did not show a defect on the FD maps. However, the FD maps were not able to pick up minor hypointense regions. In addition, since the slice thickness of the FD images was 15 mm, movements of the

TABLE 2 Qualitative MRI scoring

	Axial SPGR insp (N = 27)	Axial SPGR exp (n = 29)	T2-weighted PROPELLER (n = 29)	ZTE (n = 26)	UTE (n = 10)
Fissures	1 (1–1)	1 (1–2)	2 (2–2)	2 (2–2)	2 (2–2)
Vessels	2 (2–2)	2 (2–3)	4 (3–4)	4 (4–4)	4 (4–4)
Bronchi	2 (2–2)	2 (2–2)	3 (3–4)	4 (4–4)	4 (4–4)
Noise/artifacts	3 (2–3)	3 (2–3)	3 (3–4)	2 (2–4)	3 (3–4)
Overall acceptability	3 (2–3)	3 (2–3)	4 (3–4)	4 (3–4)	4 (4–4)

Note: Qualitative MRI scoring according to Bae et al.[23] The scores range from 1 representing worst depiction/most artifacts/worse acceptability and 5 representing best depiction of structures/least artifacts/superior acceptability (for exact scoring method see Supporting Information: 3).

Abbreviations: MRI, magnetic resonance imaging; PROPELLER, periodically rotated overlapping parallel lines with enhanced reconstruction; SPGR, spoiled gradient echo; UTE, ultrashort echo time; ZTE, zero echo time.

TABLE 3 Quantitative MRI results

	BPD (n = 11)	Preterm (n = 9)	Healthy volunteers (n = 9)	*p* Value
Free-breathing				
Diseased lung	9.1 (5.9–11.6)	3.4 (2.5–5.4)	0.4 (0.1–0.8)	**<0.001[1], <0.001[2], 0.001[3]**
Hypointensity	0.0 (0.0–0.8)	0.2 (0.0–0.3)	(0.0–0.0)	0.71[1], 0.18[2], 0.09[3]
Hyperintensity	1.8 (1.4–3.6)	0.5 (0.1–1.4)	(0.0–0.2)	**0.004[1], <0.001[2], 0.01[3]**
Bronchopathy	5.3 (4.5–7.7)	2.6 (1.6–3.7)	0.2 (0.0–0.7)	**0.002[1], <0.001[2], 0.001[3]**
Normal lung	90.9 (88.4–94.1)	96.6 (94.6–97.6)	99.6 (99.3–100.0)	**<0.001[1], <0.001[2], 0.001[3]**
Expiration				
Hypointensity	2.5 (0.0–6.2)	0.9 (0.0–0.9)	0.0 (0.0–0.0)	0.55[1], **0.03[2], 0.01[3]**
Normal lung	97.5 (93.8–100.0)	99.1 (96.5–100.0)	100.0 (100.0–100.0)	0.55[1], **0.03[2], 0.01[3]**
Architectural distortion	2 (1–2)	1 (0–1)	0 (0–0)	**0.002[1], <0.001[2], 0.01[3]**

Note: Quantitative MRI results according to the MERGE scoring and degree of architectural distortion. Data are presented as % of the total lung volume for the MERGE scoring and as a degree for architectural distortion, with 0 = none, 1 = mild, 2 = moderate, and 3 = severe. All data are presented as median (interquartile range). $p < 0.05$ is in bold, 1 = children with BPD compared to preterm-born children without BPD, 2 = children with BPD compared to healthy volunteers, and 3 = preterm-born children without BPD compared to healthy volunteers.

Abbreviations: BPD; bronchopulmonary dysplasia; MRI, magnetic resonance imaging.

chest wall and heart appeared as signal defects on the FD maps. To prevent wrongful interpretation, these defects in the paramediastinal and peripheral regions of the lungs were left out of the visual comparison. Figure 3 shows examples of the comparison between the coronal reformatted SGPR expiration sequences and FD maps.

4 | DISCUSSION

This is the first study using MRI to image structure as well as function changes of the lungs in preterm-born children with and without BPD at school age. Our findings show that MRI is capable to identify clinically relevant changes in lung structure and function in these populations. We propose chest MRI as a sensitive and safe imaging

method, without ionizing radiation, contrast agents, or the use of anesthesia, for the long-term follow-up of preterm-born children.

Using a conventional MRI protocol on a standard 1.5 Tesla scanner, we were able to identify the most common structural lung changes related to preterm birth, namely hypo- and hyperintense regions and bronchopathy.[6] Children with BPD showed a higher percentage of hyperintense regions and bronchopathy on free-breathing MRI sequences compared to preterm-born children without BPD and healthy volunteers. These findings are in line with previous research using chest CT in this population.[6,9,29,30] We also found a higher percentage of hypointense regions on the expiratory MRI sequence in children with BPD compared to preterm-born children without BPD and healthy volunteers, as shown in previous CT studies.[31]
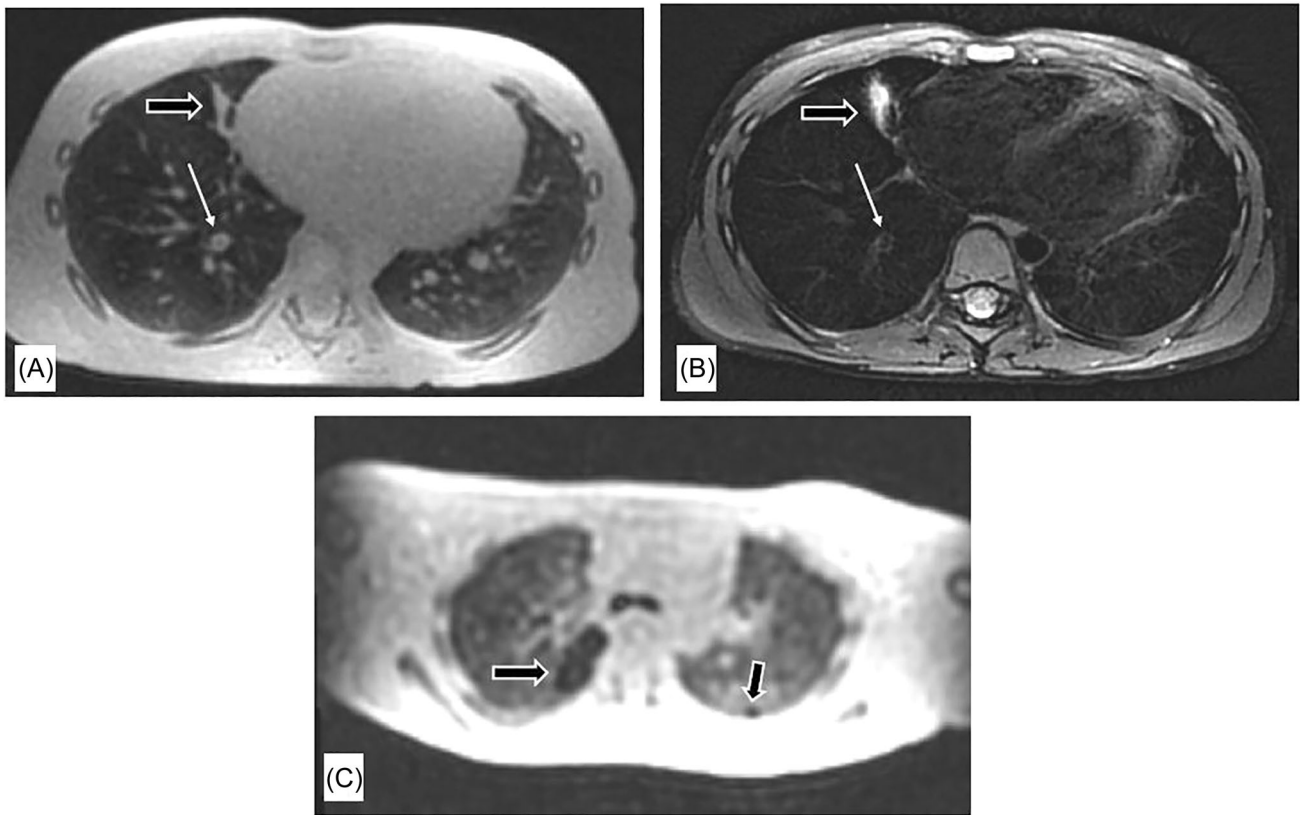
FIGURE 2 Axial 3D Proton Density weighted (PD-w) Zero echo time with navigator (ZTE vnav) (A) and axial 2D T2-weighted PROPELLER (B) and axial reconstructed 3D PD-w SPGR expiration images in an 8-year-old girl with severe BPD. Note the segmental bronchus of the right lower lobe with bronchial wall thickening (A and B, thin arrow), the hyperintense parenchymal abnormality in the middle lobe representing atelectasis/fibrosis (A and B, thick arrow), and the hypointense regions on the expiratory images (C, thick arrow).

**TABLE 4** Correlation analyses between quantitative MRI analyses and spirometry outcomes

	FEV_1 % predicted		FEV_1/FVC % predicted		FEF_{75} % predicted	
Free-breathing						
Diseased lung	r_s: 0.40 (−0.69 to −0.01)	**0.04**	r_s: −0.49 (−0.75 to −0.11)	**0.009**	r: −0.63 (−0.96 to −0.31)	**<0.001**
Hypointensity	r_s: −0.18 (−0.53–0.21)	0.36	r_s: −0.38 (−0.67–0.01)	**0.05**	r: −0.48 (−0.83 to −0.14)	**0.008**
Hyperintensity	r_s: −0.57 (−0.79 to −0.21)	**0.002**	r_s: −0.66 (−0.84 to −0.34)	**<0.001**	r: −0.73 (−1.00 to −0.45)	**<0.001**
Bronchopathy	r_s: −0.26 (−0.59 to 0.14)	0.19	r_s: −0.33 (−0.64–0.07)	0.09	r: −0.40 (−0.78 to −0.02)	**0.04**
Expiration						
Hypointensity	r_s: −0.32 (−0.63–0.07)	0.10	r_s: −0.21 (−0.63–0.08)	0.11	r: −0.38 (−0.76 to −0.01)	**0.04**
Architectural distortion	r_s: −0.63 (−0.82 to −0.29)	**<0.001**	r_s: −0.66 (−0.84 to −0.34)	**<0.001**	r: −0.77 (−1.03 to −0.51)	**<0.001**

Note: Data are presented as Pearson (*r*) or Spearman (r_s) correlation coefficient (95% confidence interval). $p < 0.05$ is in bold.

Abbreviations: FEF_{75}, forced expiratory flow at 75% of expiration; FEV_1, forced expiratory volume in 1 s; FVC, forced vital capacity; MRI, magnetic resonance imaging.

We showed significant correlations between an increase of abnormalities on MRI and lower spirometry outcomes in children with BPD. The strongest correlation was found for FEF_{75}, reflecting airflow in the peripheral airways and thereby representing small airway disease, which in previous studies has been linked to hypoattenuation on CT.[32,33] It is hypothesized that small airways disease in BPD is caused by both altered development of the alveoli and its vascularization as well as persistent airway inflammation and smooth muscle hypertrophy, and shows the link with the predisposition of developing the chronic obstructive pulmonary disease later in life for preterm-born children.[34,35]
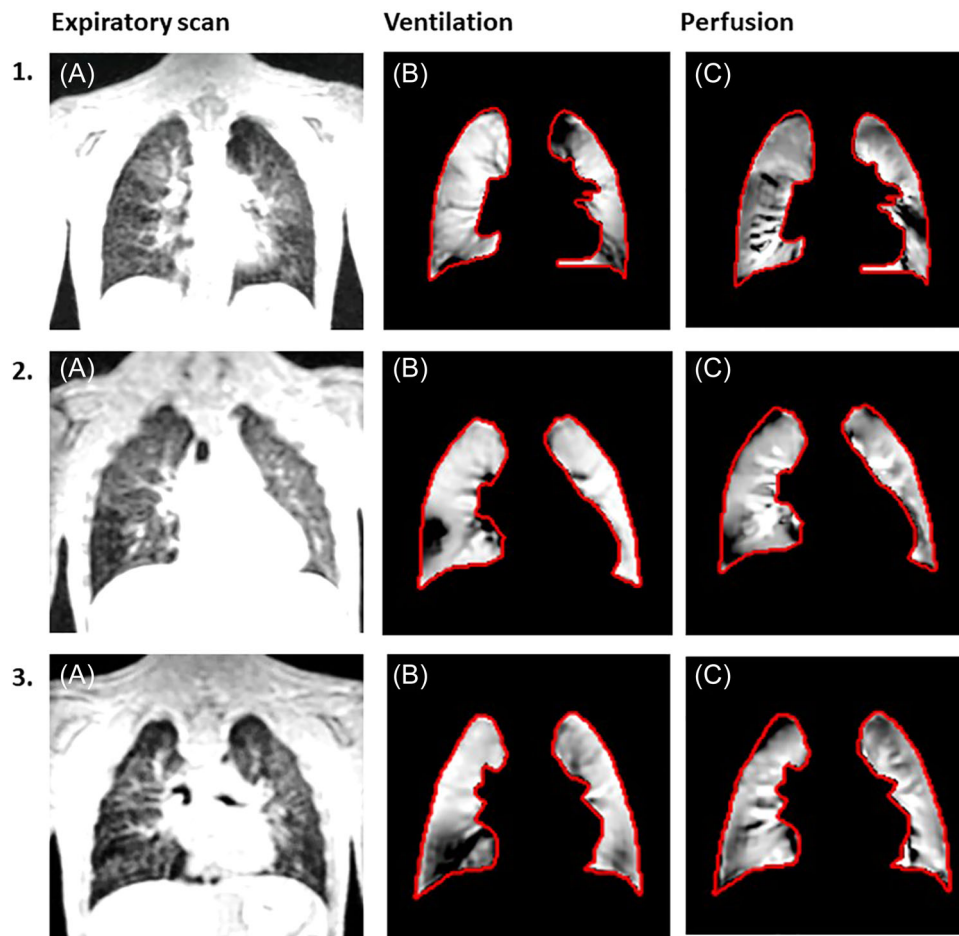
FIGURE 3 Example images of the comparison between the expiratory MRI scans and FD ventilation and perfusion maps. Black on the FD maps corresponds to a defect. (1) Coronal reformat SPGR expiration image showing hypointense regions in the right lower lobe and apical part of the left lung (A), corresponding FD ventilation map showing a defect in the apical part of the left lung (B), and FD perfusion map showing a defect in the right lower lobe (C) in a child with BPD. (2) Coronal reformat SPGR expiration image showing a hypointense region in the right lower lobe (A), corresponding FD ventilation map showing a defect in the right lower lobe (B), and FD perfusion map showing a defect in the right lower lobe (C) in a child with BPD. (3) Coronal reformat SPGR expiration image showing a hypointense region in the right lower lobe (A), corresponding FD ventilation map showing a defect in the right lower lobe (B), and FD perfusion map showing no defect (C) map in a child with BPD. BPD, bronchopulmonary dysplasia; FD, Fourier Decomposition; MRI, magnetic resonance imaging; SPGR, spoiled gradient echo. [Color figure can be viewed at wileyonlinelibrary.com]

A unique feature of our study is that we included preterm-born children without BPD. Preterm-born children without BPD showed significantly better spirometry outcomes compared to preterm children with BPD, but no difference with healthy volunteers. Lower spirometry values in children with BPD compared to preterm-born children without BPD have been previously described.[36,37] In addition, studies show a further decrease in lung function over time in preterm-born children with and without BPD and a correlation between this decrease in lung function and increased bronchial wall thickening on CT, suggesting the presence of airway inflammation in this population.[4,5] Although we did not find a lower spirometry outcome in our cohort of preterm-born children without BPD, we did find a significantly higher percentage of abnormalities on MRI compared to healthy volunteers. These findings indicate that MRI might be able to pick up minor changes in lung structure and function that are not detected with spirometry.

Our findings on structural lung changes in both preterm-born children with and without BPD bring up the validity and clinical importance of the currently used diagnostic criteria of the severity of BPD, which is based on the amount of oxygen need at 36 weeks PMA.[38] Lung abnormalities in preterm-born children are linear and therefore the current diagnostic (severity) criteria, set at one moment in time, and dividing patients into a categorical severity scale do not necessarily identify those children at risk and in need of further follow-up. A recent neonatal study showed MRI findings to be a better predictor of short-term clinical outcomes than BPD severity score according to the NHI criteria.[18] Although long-term follow-up on these findings is necessary, these data indicate that imaging might

aid in identifying those preterm patients at risk for respiratory morbidity.

The use of chest CT for the radiological follow-up of lung abnormalities in preterm-born children has the advantage that protocols are easier to standardize across centers and vendors compared to MRI and radiation doses are coming down progressively, also thanks to the introduction of photon counting CT technology.[39] Though, the risk for scanning neonatal patients who are more sensitive to radiation should still be taken into consideration.[40,41] In addition, MRI has the additional benefit of functional imaging. In this study, we explored the use of FD to identify hypointense regions as ventilation or perfusion defects and found this method to be well capable of classifying large hypointense regions. However, our algorithm was not yet sensitive enough to identify minor hypointense regions, such as mosaic perfusion, especially at the periphery of the lung. The distinction between ventilation or perfusion defects on imaging is of special interest in the BPD population, where a simplified development of the alveoli can be associated with pulmonary vascular diseases, such as hypoperfusion and pulmonary hypertension.[42] Future research should focus on the improvement of the FD sequence and postprocessing.

Based on our qualitative scoring, we recommend the use of an MRI protocol consisting of both T2 weighted sequences (such as our PROPELLER sequence) to identify bronchopathy, in combination with a short TE sequence (such as ZTE/UTE) and an end-expiratory SPGR sequence to identify hypointense regions. Some of these short TE sequences have the additional benefit of being silent which makes the MRI less burdensome for (young) children. Hyperintense regions are easily identified on both sequences. We were not able to identify a difference in hypointense regions on free-breathing sequences between all groups, as has been previously described in CT studies.[9,29–31] However, using end-expiratory breath-hold imaging, children with BPD showed a significant higher amount of hypointense regions compared to healthy volunteers. This can be explained by the better contrast-to-noise ratio seen on MRI at residual volume using expiratory sequences, compared to the functional residual capacity volume obtained in free-breathing sequences. Therefore, we recommend expiratory sequences at residual volume level for the identification of hypointense regions. This implies that in younger children with BPD, who may not be able to perform breath-hold imaging, detection of the hypointense region might not be feasible or cumbersome.

Our study has a few limitations. First, being our primary aim to develop the MRI protocol, our study was only conducted in a small population, and not all BPD severity groups (mild or moderate BPD) were included, therefore our findings should be validated in a larger group of patients. Second, we lacked clinical information, such as respiratory symptoms, comorbidities, and use of medication, to correlate with MRI findings. Finally, we did not have CT available for comparison.

5 | CONCLUSION

In conclusion, we show that MRI has the potential to safely image structural and functional abnormalities of the lungs at school-age in preterm-born children with and without BPD. An increase in MRI abnormalities correlates with lower spirometry outcomes. These results support the importance of including imaging in the long-term follow-up of all preterm-born children to identify those children at risk for respiratory morbidity and therefore in need of closer monitoring. Future research in premature-born children should focus on long-term follow-up of structural and functional abnormalities, including imaging, and their relationship with lung function and clinical status. The development of our MRI protocol is the first step for a safe long-term follow-up of premature-born children.

AUTHORS CONTRIBUTIONS

Bernadette B. L. J. Elders contributed to the design of the work, data collection, data analyses, and wrote the main manuscript. Harm A. W. M. Tiddens, Mariëlle W. H. Pijnenburg, and Irwin K. M. Reiss contributed to the design of the work, critically revised the manuscript, and gave approval to the final version of the manuscript. Piotr A. Wielopolski contributed to the data collection, critically revised the manuscript, and gave approval to the final version of the manuscript. Pierluigi Ciet contributed to the design of the work, data analyses, critically revised the manuscript, and gave approval to the final version of the manuscript.

CONFLICT OF INTEREST

The authors declare no conflict of interest.

DATA AVAILABILITY STATEMENT

The data that support the findings of this study are available from the corresponding author upon reasonable request.

ORCID

Bernadette B. L. J. Elders http://orcid.org/0000-0001-5917-2147
Harm A. W. M. Tiddens https://orcid.org/0000-0001-5628-6667
Mariëlle W. H. Pijnenburg http://orcid.org/0000-0003-4291-468X

REFERENCES

1. Kinsella JP, Greenough A, Abman SH. Bronchopulmonary dysplasia. Lancet. 2006;367(9520):1421-1431.
2. Islam JY, Keller RL, Aschner JL, Hartert TV, Moore PE. Understanding the short- and long-term respiratory outcomes of prematurity and bronchopulmonary dysplasia. Am J Respir Crit Care Med. 2015;192(2):134-156.
3. Voynow JA. "New" bronchopulmonary dysplasia and chronic lung disease. Paediatr Respir Rev. 2017;24:17-18.

4. Simpson SJ, Turkovic L, Wilson AC, et al. Lung function trajectories throughout childhood in survivors of very preterm birth: a longitudinal cohort study. *Lancet Child Adolesc Health*. 2018;2(5): 350-359.

5. Simpson SJ, Logie KM, O'dea CA, et al. Altered lung structure and function in mid-childhood survivors of very preterm birth. *Thorax*. 2017;72(8):702-711.

6. van Mastrigt E, Logie K, Ciet P, et al. Lung CT imaging in patients with bronchopulmonary dysplasia: a systematic review. *Pediatr Pulmonol*. 2016;51(9):975-986.

7. Oppenheim C, Mamou-Mani T, Sayegh N, de Blic J, Scheinmann P, Lallemand D. Bronchopulmonary dysplasia: value of CT in identifying pulmonary sequelae. *AJR Am J Roentgenol*. 1994;163(1): 169-172.

8. Sung TJ, Hwang SM, Kim MY, Park SG, Choi KY. Relationship between clinical severity of "new" bronchopulmonary dysplasia and HRCT abnormalities in VLBW infants. *Pediatr Pulmonol*. 2018;53(10): 1391-1398.

9. van Mastrigt E, Kakar E, Ciet P, et al. Structural and functional ventilatory impairment in infants with severe bronchopulmonary dysplasia. *Pediatr Pulmonol*. 2017;52(8):1029-1037.

10. Duijts L, van Meel ER, Moschino L, et al. European Respiratory Society guideline on long-term management of children with bronchopulmonary dysplasia. *Eur Respir J*. 2020;55(1):1900788.

11. Ciet P, Tiddens HA, Wielopolski PA, et al. Magnetic resonance imaging in children: common problems and possible solutions for lung and airways imaging. *Pediatr Radiol*. 2015;45(13): 1901-1915.

12. Hatabu H, Ohno Y, Gefter WB, et al. Expanding applications of pulmonary MRI in the clinical evaluation of lung disorders: Fleischner Society position paper. *Radiology*. 2020;297(2):286-301.

13. Flors L, Mugler JP, 3rd, Paget-Brown A, et al. Hyperpolarized Helium-3 diffusion-weighted magnetic resonance imaging detects abnormalities of lung structure in children with bronchopulmonary dysplasia. *J Thorac Imaging*. 2017;32(5):323-332.

14. Walkup LL, Tkach JA, Higano NS, et al. Quantitative magnetic resonance imaging of bronchopulmonary dysplasia in the neonatal intensive care unit environment. *Am J Respir Crit Care Med*. 2015;192(10):1215-1222.

15. Walkup LL, Woods JC. Newer imaging techniques for bronchopulmonary dysplasia. *Clin Perinatol*. 2015;42(4):871-887.

16. Higano NS, Fleck RJ, Spielberg DR, et al. Quantification of neonatal lung parenchymal density via ultrashort echo time MRI with comparison to CT. *J Magn Reson Imaging*. 2017;46(4): 992-1000.

17. Higano NS, Hahn AD, Tkach JA, et al. Retrospective respiratory self-gating and removal of bulk motion in pulmonary UTE MRI of neonates and adults. *Magn Reson Med*. 2017;77(3): 1284-1295.

18. Higano NS, Spielberg DR, Fleck RJ, et al. Neonatal pulmonary magnetic resonance imaging of bronchopulmonary dysplasia predicts short-term clinical outcomes. *Am J Respir Crit Care Med*. 2018;198(10):1302-1311.

19. Jobe AH, Bancalari E. Bronchopulmonary dysplasia. *Am J Respir Crit Care Med*. 2001;163(7):1723-1729.

20. Miller MR, Crapo R, Hankinson J, et al. General considerations for lung function testing. *Eur Respir J*. 2005;26(1):153-161.

21. Beydon N, Davis SD, Lombardi E, et al. An official American Thoracic Society/European Respiratory Society statement: pulmonary function testing in preschool children. *Am J Respir Crit Care Med*. 2007;175(12):1304-1345.

22. Quanjer PH, Hall GL, Stanojevic S, Cole TJ, Stocks J, Global Lungs Initiative. Age- and height-based prediction bias in spirometry reference equations. *Eur Respir J*. 2012;40(1):190-197.

23. Bae K, Jeon KN, Hwang MJ, et al. Comparison of lung imaging using three-dimensional ultrashort echo time and zero echo time sequences: preliminary study. *Eur Radiol*. 2019;29(5): 2253-2262.

24. Rosenow T, Oudraad MC, Murray CP, et al. PRAGMA-CF. A quantitative structural lung disease computed tomography outcome in young children with cystic fibrosis. *Am J Respir Crit Care Med*. 2015;191(10):1158-1165.

25. Loeve M, van Hal PT, Robinson P, et al. The spectrum of structural abnormalities on CT scans from patients with CF with severe advanced lung disease. *Thorax*. 2009;64(10):876-882.

26. Voskrebenzev A, Gutberlet M, Becker L, Wacker F, Vogel-Claussen J. Reproducibility of fractional ventilation derived by Fourier decomposition after adjusting for tidal volume with and without an MRI compatible spirometer. *Magn Reson Med*. 2016;76(5):1542-1550.

27. Voskrebenzev A, Gutberlet M, Kaireit TF, Wacker F, Vogel-Claussen J. Low-pass imaging of dynamic acquisitions (LIDA) with a group-oriented registration (GOREG) for proton MR imaging of lung ventilation. *Magn Reson Med*. 2017;78(4):1496-1505.

28. Voskrebenzev A, Gutberlet M, Klimeš F, et al. Feasibility of quantitative regional ventilation and perfusion mapping with phase-resolved functional lung (PREFUL) MRI in healthy volunteers and COPD, CTEPH, and CF patients. *Magn Reson Med*. 2018;79(4): 2306-2314.

29. Aukland SM, Rosendahl K, Owens CM, Fosse KR, Eide GE, Halvorsen T. Neonatal bronchopulmonary dysplasia predicts abnormal pulmonary HRCT scans in long-term survivors of extreme preterm birth. *Thorax*. 2009;64(5):405-410.

30. Wong PM, Lees AN, Louw J, et al. Emphysema in young adult survivors of moderate-to-severe bronchopulmonary dysplasia. *Eur Respir J*. 2008;32(2):321-328.

31. Aquino SL, Schechter MS, Chiles C, Ablin DS, Chipps B, Webb WR. High-resolution inspiratory and expiratory CT in older children and adults with bronchopulmonary dysplasia. *AJR Am J Roentgenol*. 1999;173(4):963-967.

32. Konstantinos Katsoulis K, Kostikas K, Kontakiotis T. Techniques for assessing small airways function: possible applications in asthma and COPD. *Respir Med*. 2016;119:e2-e9.

33. McNulty W, Usmani OS. Techniques of assessing small airways dysfunction. *Eur Clin Respir J*. 2014;1:1. Techniques of assessing small airways dysfunction - PMC (nih.gov)

34. McGrath-Morrow SA, Collaco JM. Bronchopulmonary dysplasia: what are its links to COPD. *Ther Adv Respir Dis*. 2019;13: 1753466619892492.

35. Collaco JM, McGrath-Morrow SA. Bronchopulmonary dysplasia as a determinant of respiratory outcomes in adult life. *Pediatr Pulmonol*. 2021;56(11):3464-3471.

36. Verheggen M, Wilson AC, Pillow JJ, Stick SM, Hall GL. Respiratory function and symptoms in young preterm children in the contemporary era. *Pediatr Pulmonol*. 2016;51(12):1347-1355.

37. Broström EB, Thunqvist P, Adenfelt G, Borling E, Katz-Salamon M. Obstructive lung disease in children with mild to severe BPD. *Respir Med*. 2010;104(3):362-370.

38. Bancalari E, Jain D. Bronchopulmonary dysplasia: can we agree on a definition? *Am J Perinatol*. 2018;35(6):537-540.

39. Willemink MJ, Persson M, Pourmorteza A, Pelc NJ, Fleischmann D. Photon-counting CT: technical principles and clinical prospects. *Radiology*. 2018;289(2):293-312.

40. Brenner D, Elliston C, Hall E, Berdon W. Estimated risks of radiation-induced fatal cancer from pediatric CT. *AJR Am J Roentgenol*. 2001;176(2):289-296.

41. Pearce MS, Salotti JA, Little MP, et al. Radiation exposure from CT scans in childhood and subsequent risk of leukaemia and brain

—WILEY—| 11

tumours: a retrospective cohort study. *Lancet*. 2012;380(9840): 499-505.

42. Parker TA, Abman SH. The pulmonary circulation in bronchopulmonary dysplasia. *Semin Neonatol*. 2003;8(1):51-61.

SUPPORTING INFORMATION

Additional supporting information can be found online in the Supporting Information section at the end of this article.